JOURNAL OF APPLIED CRYSTALLOGRAPHY

ISSN: 1600-5767
journals.iucr.org/j

A remark on *ab initio* indexing of electron backscatter diffraction patterns

Adam Morawiec

J. Appl. Cryst. (2021). **54**, 1844–1846

JOURNAL OF APPLIED CRYSTALLOGRAPHY

ISSN 1600-5767

A remark on *ab initio* indexing of electron backscatter diffraction patterns

Adam Morawiec*

Polish Academy of Sciences, Institute of Metallurgy and Materials Science, Reymonta 25, 30-059 Krakow, Poland.
*Correspondence e-mail: nmmorawi@cyf-kr.edu.pl

Received 18 June 2021
Accepted 7 September 2021

Edited by A. Barty, DESY, Hamburg, Germany

Keywords: crystal diffraction; indexing; electron backscatter diffraction; EBSD; lattice parameters.

Supporting information: this article has supporting information at journals.iucr.org/j

There is a growing interest in *ab initio* indexing of electron backscatter diffraction (EBSD) patterns. The methods of solving the problem are presented as innovative. The purpose of this note is to point out that *ab initio* EBSD indexing belongs to the field of indexing single-crystal diffraction data, and it is solved on the same principles as indexing of patterns of other types. It is shown that reasonably accurate EBSD-based data can be indexed by programs designed for X-ray data.

1. Introduction

A number of papers have recently been published on determination of lattice parameters based on electron backscatter diffraction (EBSD) patterns (Dingley & Wright, 2009; Li *et al.*, 2014; Li & Han, 2015; Han *et al.*, 2018; Ming *et al.*, 2018; Han & Zhao, 2018; Oishi-Tomiyasu *et al.*, 2021; Nolze *et al.*, 2021). The process can be seen as semi-automatic *ab initio* indexing. The papers consider the problem in nearly complete detachment from other single-crystal indexing methods.

The indexing of single-crystal diffraction patterns is a step in crystal structure determination, and it has been studied from various viewpoints for many years. In particular, many efforts have been made to create efficient and robust software for automatic indexing of X-ray diffraction data: see Duisenberg (1992), Carr *et al.* (1992), Kabsch (1993, 2010), Ravelli *et al.* (1996), Otwinowski & Minor (1997), Campbell (1998), Powell (1999), Pflugrath (1999), Pilz *et al.* (2002), Leslie *et al.* (2002), Sauter *et al.* (2004), Tamura (2014), Morawiec (2017, 2021) and Gevorkov *et al.* (2019) for selected accounts from the past three decades. There is a question whether the *ab initio* indexing of EBSD patterns is so different that it needs to be investigated as a separate crystallographic problem. Does it require a distinct formalism? Is it justified to portray *ab initio* EBSD indexing as a previously unconsidered issue? The answers to these questions are negative. One could scrutinize particular steps of EBSD indexing and indicate their analogs in other indexing procedures, but it is easier to prove the similitude simply by showing that EBSD data can be indexed by programs designed for single-crystal X-ray data.

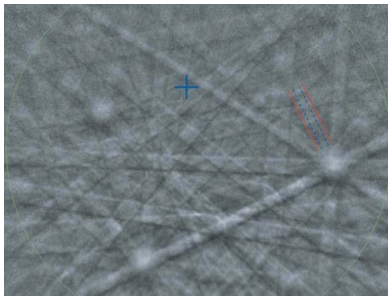

2. Example data

Briefly, an EBSD pattern consists of diffraction bands. Blurred band edges are low-curvature conics. They correspond to nodes of the reciprocal lattice of the diffracting crystal. For more on the geometry of formation of EBSD patterns see, for example, Dingley & Wright (2009) or Ming *et al.* (2018).

For illustration, the experimental EBSD pattern shown in Fig. 1 is used. It is suitable for comparisons because its original version was meticulously analyzed by Li & Han (2015). That paper also provides all data needed to process the pattern: the radiation wavelength λ, the pattern center, and the ratio of the pattern width and the source-to-detector distance. For our test, edges of 26 bands indexed by Li & Han (2015) were marked manually by visual inspection, without any band-profile model. The dimensions of the pattern were 499×380 pixels, and the screen resolution was 1680×1050 pixels. The positions of the edges were used to get the scattering vectors $\mathbf{H}_i$ ($i = 1, 2, \ldots, 26$). For a given band, the scattering vector is $\mathbf{H} = (\widehat{\mathbf{k}}_1 - \widehat{\mathbf{k}}_2)/\lambda$, where $\widehat{\mathbf{k}}_j$ ($j = 1, 2$) is the unit vector directed toward the foot of the perpendicular from the pattern center of the jth edge (see Fig. 2 and the supplementary material). It is quite obvious that, owing to the small Bragg angles, the magnitudes of the vectors $\mathbf{H}_i$ are affected by relatively large errors.

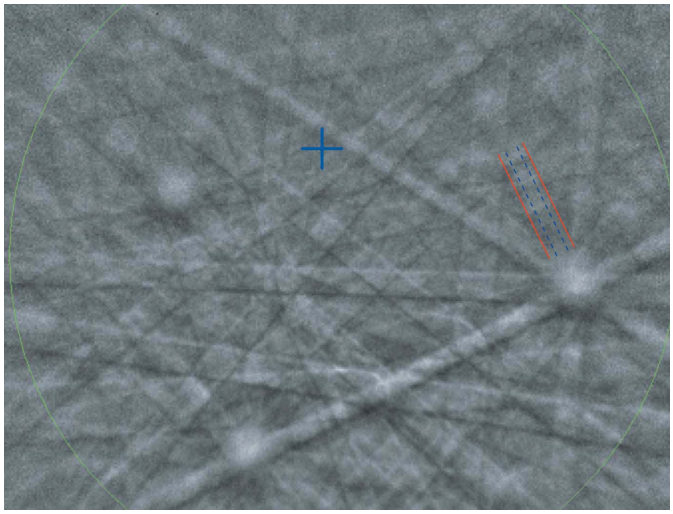

Figure 1
Experimental EBSD pattern of a mineral (diopside) published by Li & Han (2015). The cross marks the location of the pattern center. Approximate positions of edges of the band No. 24 used by Li & Han (2015) are marked by dashed blue lines and those used here by continuous red lines.

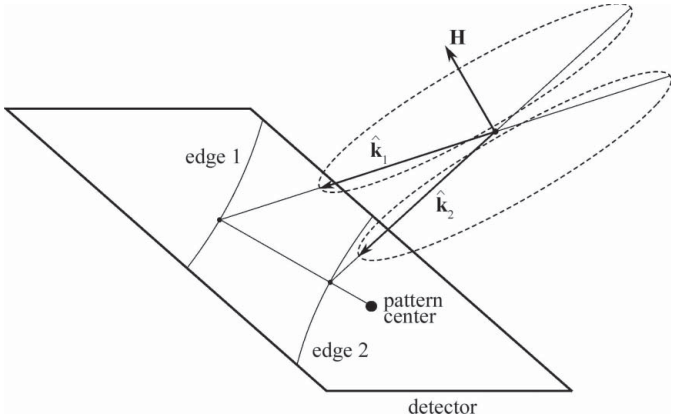

Figure 2
Schematic illustration of the configuration of edges of an EBSD band, $\widehat{\mathbf{k}}_j$ vectors and the scattering vector $\mathbf{H}$.

3. Indexing with software for monochromatic X-ray data

The example EBSD data were processed by the programs *DirAx* (Duisenberg, 1992) and *Ind_X* (Morawiec, 2017), designed for indexing diffraction patterns obtained from monochromatic radiation sources. Both *DirAx* and *Ind_X* accept the scattering vectors $\mathbf{H}_i$ as the input data, both search for a reciprocal lattice matching these vectors, and both are available on the internet. *DirAx* is at http://www.crystal.chem.uu.nl/distr/dirax/, and *Ind_X* can be downloaded from http://imim.pl/personal/adam.morawiec/.

The solutions for the example data were obtained without any elaborate processing. Knowing that the vector magnitudes are inaccurate, relatively large tolerances were allowed. *DirAx* indexed 16 bands, and the remaining ten were ignored as non-fitting reflections. *Ind_X* indexed 19 reflections. Both programs indexed the data correctly in the sense that the solutions were equivalent to that given by Li & Han (2015). [The only exception was the band No. 24 with indices resulting from *Ind_X* twice those listed by Li & Han (2015); the band marked for this study turned out to be broader than that used by Li & Han (2015).] The supplementary material contains the *DirAx* and *Ind_X* input and output files, and the relationships between reflection indices listed by Li & Han (2015) and those obtained using *DirAx* and *Ind_X*.

4. Indexing with software for Laue patterns

The large errors of magnitudes of the scattering vectors affect conventional indexing. If the magnitudes are discarded by normalizing the vectors, the problem becomes analogous to *ab initio* indexing of Laue diffraction patterns (Carr *et al.*, 1992; Ravelli *et al.*, 1996; Tamura, 2014). The prototype Laue indexer *IndX_Laue* introduced by Morawiec (2021) was applied to the example data. The input of *IndX_Laue* consists of normalized scattering vectors $\widehat{\mathbf{H}}_i = \mathbf{H}_i/|\mathbf{H}_i|$, and the program is available at the same internet location as *Ind_X*. With a large extent of the search for the solution, the program indexed all 26 reflections.

Ab initio indexing of normalized scattering vectors provides only relative dimensions of the lattice, *i.e.* the absolute volume of the primitive cell is indeterminable [see *e.g.* the article by Carr *et al.* (1992)]. Moreover, there are no grounds for specifying the order of a reflection, and only relatively prime indices are ascribed to reflections. However, having also crude estimates of the magnitudes of the scattering vectors, one can fit the scaling factor and the orders of the indexed reflections. An algorithm for that is given in Appendix *A*. Application of the algorithm to the example data gave an indexing solution equivalent to that obtained using *DirAx* and *Ind_X*, apart from the fact that all reflections were indexed. See the supplementary material for details.

5. Concluding remarks

Indexing of EBSD patterns is closely related to indexing of other single-crystal data. EBSD patterns can be indexed by

software designed for X-ray data. This was demonstrated using computer programs convenient for the author, but other tools could have been applied for that purpose.

The problem of *ab initio* EBSD indexing is similar to indexing pink-beam data. In both cases, the directions of the scattering vectors are relatively accurate, whereas their magnitudes are uncertain. For pink-beam data, the ranges of the uncertainties are related to the spectral width of the radiation, and in the case of EBSD-based data, they are linked to inaccuracies of band widths. Like EBSD patterns, some pink-beam X-ray data are indexed using software designed for monochromatic data [see *e.g.* Martin-Garcia *et al.* (2019) and Tolstikova (2020)].

We stress that this note is not to advocate indexing EBSD patterns with software for X-ray data. Each diffraction method has a specific geometry, it is convenient to analyze particular geometries using dedicated interfaces, and all new software for processing EBSD patterns will be appreciated. The main message here is that dealing with *ab initio* EBSD indexing does not require starting from scratch. One can take advantage of the experience gained in indexing diffraction patterns of other types. Considering the EBSD indexing problem in isolation from existing indexing methods hinders the diffusion of ideas and increases the fragmentation of the research field. There is a significant cost of ignoring the bigger picture and duplicating past efforts (Daughton, 2001).

APPENDIX *A*
Algorithm for determining the scaling factor

Let D be a matrix with direct basis vectors (in rows) in the Cartesian laboratory reference frame. [D is the inverse of the **UB** matrix of Busing & Levy (1967).] The basis resulting from indexing normalized scattering vectors is known except for a scaling factor; with the factor denoted by S (> 0), one has the matrix $\Delta = D/S$ such that $|\det \Delta| = 1$. The true volume of the direct lattice cell is $V = |\det D| = S^3$. Let $\mathtt{h}_i$ in typewriter font denote the column matrix with relatively prime indices of the ith reflection. The relationship between the scattering vector $\mathbf{H}_i$ and its indices $\mathtt{h}_i$ is $D\,\mathbf{H}_i = S\,\Delta\,\mathbf{H}_i \simeq m_i\,\mathtt{h}_i$, where $m_i \geq 1$ is a small integer. With $\check{\mathbf{h}}_i = \Delta^{-1}\,\mathtt{h}_i$, one has

$$S\,\mathbf{H}_i \simeq m_i\,\check{\mathbf{h}}_i. \qquad (1)$$

Given N indexed scattering vectors $\mathbf{H}_i$ and corresponding vectors $\check{\mathbf{h}}_i$, from the above relationship, one can determine the common factor S and the orders m_i of individual reflections by the following procedure.

Consider a selected reflection j (*i.e.* a selected $\mathbf{H}_j$ and $\check{\mathbf{h}}_j$), assuming that $m_j = 1$:

(1) Get the scaling factor σ_j of the jth reflection by minimizing $|\sigma\,\mathbf{H}_j - \check{\mathbf{h}}_j|^2$ with respect to σ; it is given by $\sigma_j = \mathbf{H}_j \cdot \check{\mathbf{h}}_j / |\mathbf{H}_j|^2$.

(2) With the obtained σ_j, for each $i = 1, 2, \ldots, N$, get the integer factor $\mu_i(j) \geq 1$ by minimizing $|\sigma_j\,\mathbf{H}_i - \mu\,\check{\mathbf{h}}_i|^2$ with respect to μ; it is given by $\mu_i(j) = \max(1,\ \lfloor \sigma_j\,\mathbf{H}_i \cdot \check{\mathbf{h}}_i / |\check{\mathbf{h}}_i|^2 \rceil)$, where $\lfloor x \rceil$ denotes the integer nearest to x.

(3) Knowing $\mu_i(j)$ for $i = 1, 2, \ldots, N$, compute the scaling factor $\Sigma(j)$ applicable to all indexed reflections by minimizing $\sum_{i=1}^{N} |\sigma\,\mathbf{H}_i - \mu_i(j)\,\check{\mathbf{h}}_i|^2$ with respect to σ; it is given by

$$\Sigma(j) = \frac{\sum_{i=1}^{N} \mu_i(j)\,\mathbf{H}_i \cdot \check{\mathbf{h}}_i}{\sum_{i=1}^{N} |\mathbf{H}_i|^2}. \qquad (2)$$

(4) Compute $R(j) = \sum_{i=1}^{N} |\Sigma(j)\,\mathbf{H}_i - \mu_i(j)\,\check{\mathbf{h}}_i|^2$.

Since the initial assumption $m_j = 1$ may be false, steps 1–4 must be repeated for all $j = 1, \ldots, N$ (or at least for a sufficient number of them). The actual scaling factor S corresponds to $j = J$ leading to minimal R, *i.e.* with $J = \arg\min_j R(j)$, one has $S = \Sigma(J)$ and $m_i = \mu_i(J)$. The actual indices of the ith reflection are $m_i\,\mathtt{h}_i$.

References

Busing, W. R. & Levy, H. A. (1967). *Acta Cryst.* **22**, 457–464.
Campbell, J. W. (1998). *J. Appl. Cryst.* **31**, 407–413.
Carr, P. D., Cruickshank, D. W. J. & Harding, M. M. (1992). *J. Appl. Cryst.* **25**, 294–308.
Daughton, C. G. (2001). *Environ. Forensics*, **2**, 277–282.
Dingley, D. J. & Wright, S. I. (2009). *J. Appl. Cryst.* **42**, 234–241.
Duisenberg, A. J. M. (1992). *J. Appl. Cryst.* **25**, 92–96.
Gevorkov, Y., Yefanov, O., Barty, A., White, T. A., Mariani, V., Brehm, W., Tolstikova, A., Grigat, R.-R. & Chapman, H. N. (2019). *Acta Cryst.* A**75**, 694–704.
Han, M., Chen, C., Zhao, G., Li, L., Nolze, G., Yu, B., Huang, X. & Zhu, Y. (2018). *Acta Cryst.* A**74**, 630–639.
Han, M. & Zhao, G. (2018). *Microsc. Microanal.* **24**, 670–671.
Kabsch, W. (1993). *J. Appl. Cryst.* **26**, 795–800.
Kabsch, W. (2010). *Acta Cryst.* D**66**, 125–132.
Leslie, A. G. W., Powell, H. R., Winter, G., Svensson, O., Spruce, D., McSweeney, S., Love, D., Kinder, S., Duke, E. & Nave, C. (2002). *Acta Cryst.* D**58**, 1924–1928.
Li, L. & Han, M. (2015). *J. Appl. Cryst.* **48**, 107–115.
Li, L., Ouyang, S., Yang, Y. & Han, M. (2014). *J. Appl. Cryst.* **47**, 1466–1468.
Martin-Garcia, J. M., Zhu, L., Mendez, D., Lee, M.-Y., Chun, E., Li, C., Hu, H., Subramanian, G., Kissick, D., Ogata, C., Henning, R., Ishchenko, A., Dobson, Z., Zhang, S., Weierstall, U., Spence, J. C. H., Fromme, P., Zatsepin, N. A., Fischetti, R. F., Cherezov, V. & Liu, W. (2019). *IUCrJ*, **6**, 412–425.
Ming, H., Guangming, Z. & Ye, Z. (2018). *Ultramicroscopy*, **195**, 136–146.
Morawiec, A. (2017). *J. Appl. Cryst.* **50**, 647–650.
Morawiec, A. (2021). *J. Appl. Cryst.* **54**, 333–337.
Nolze, G., Tokarski, T., Rychłowski, Ł., Cios, G. & Winkelmann, A. (2021). *J. Appl. Cryst.* **54**, 1012–1022.
Oishi-Tomiyasu, R., Tanaka, T. & Nakagawa, J. (2021). *J. Appl. Cryst.* **54**, 624–635.
Otwinowski, Z. & Minor, W. (1997). *Methods Enzymol.* **276**, 307–326.
Pflugrath, J. W. (1999). *Acta Cryst.* D**55**, 1718–1725.
Pilz, K., Estermann, M. & van Smaalen, S. (2002). *J. Appl. Cryst.* **35**, 253–260.
Powell, H. R. (1999). *Acta Cryst.* D**55**, 1690–1695.
Ravelli, R. B. G., Hezemans, A. M. F., Krabbendam, H. & Kroon, J. (1996). *J. Appl. Cryst.* **29**, 270–278.
Sauter, N. K., Grosse-Kunstleve, R. W. & Adams, P. D. (2004). *J. Appl. Cryst.* **37**, 399–409.
Tamura, N. (2014). *Strain and Dislocation Gradients From Diffraction*, edited by R. Barabash & G. Ice, pp. 125–155. London: Imperial College Press.
Tolstikova, A. (2020). PhD thesis, Universität Hamburg, Germany.

Supplementary material

to the paper 'A remark on *ab initio* indexing of EBSD patterns' by A. Morawiec

This file contains results of indexing of the example EBSD pattern shown in Fig. 1. Input and output files of *DirAx*, *Ind_X* and *IndX_Laue* are in Tables 2–7. For convenience, the reflection indices listed in [1] are repeated in Table 1.

At the end, there is a derivation of the formula for determination of scattering vectors from positions of edges of EBSD bands.

Table 1: Reflection indices $\mathtt{h}_{Li}$ listed in [1].

	h	k	l
1	31	−20	−2
2	−12	7	1
3	−29	18	2
4	−43	28	3
5	6	−4	0
6	37	−24	−2
7	−25	16	2
8	6	−3	0
9	−24	16	2
10	−13	9	1
11	1	0	0
12	0	1	0
13	96	−61	−6
14	55	−36	−3
15	−6	4	1
16	0	0	1
17	−6	3	1
18	48	−31	−3
19	46	−29	−3
20	−44	28	3
21	−41	26	3
22	23	−14	−1
23	84	−54	−5
24	34	−22	−2
25	7	−4	0
26	12	−7	0

Table 2: *DirAx* input file. The parameters of the program are given in the first five commented lines. The wavelength (1.54056Å) is not used in computations. The following lines contain Cartesian components (in Å^{-1}) of the scattering vectors $\boldsymbol{H}_i$ ($i = 1, 2, \ldots, 26$).

```
!  LevelFit:   1/100 [1/A]
!  maximal D: 15A
!  IndexFitFactor:      3.00
!  Delta axes zero :    0.1A
!  Delta angles zero :  0.2deg
   1.54056
   -0.381613    0.245448   -0.040362
   -0.413404   -0.507353    0.056016
    0.444278    0.351223    0.001019
   -0.508321    0.399310    0.078563
   -0.317655   -0.161782    0.195319
   -0.027002   -0.373507    0.238714
    0.588358   -0.022478   -0.159996
    0.174490   -0.628767   -0.254487
   -0.578591    0.535110    0.240619
    0.199885   -0.604781   -0.115379
   -0.055426   -0.603809   -0.087438
    0.178921    0.911853    0.068243
    0.825259    0.142683    0.231164
   -0.068180   -0.788425    0.309236
   -0.610669    0.098132    0.320284
    0.908075    0.061048   -0.502669
    0.775171    0.699036   -0.265922
    0.331995   -0.301704    0.086418
    0.540518    0.253031    0.062502
    0.580123    0.047910   -0.021023
    0.577995    0.087090   -0.081528
    0.103485   -0.482924   -0.312692
    0.382132   -0.344033    0.269722
    0.251451   -0.502520    0.235751
   -0.262867    0.326993    0.256804
    0.476508   -0.461288   -0.440052
```

Table 3: *DirAx* output file.

```
results from DIRAX for EBSD_DAT                    Friday 21 May 2021 - 10:17:09
================================================================================
Lambda: 1.54056  LevelFit: 1/100  IndexFitFactor: 3.00
IndexFit = LevelFit*IndexFitFactor = (1/100)*3.00 = 1/33
Dmax: 15  Acceptance Level (ACL): 19
--------------------------------------------------------------------------------
 nr      h       k       l     theta    phib    chib     dth      dom      dch
--------------------------------------------------------------------------------
 1=N  -1.379  -0.045  -2.662   20.54   57.25   -5.08
 2 H  -2.947  -1.981   0.904   30.39  140.83    4.89   -0.862   -0.843   -0.605
 3=N   2.767   1.834   0.058   25.86  -51.67    0.10
 4=N  -1.841   0.862  -3.590   30.10   51.85    6.93
 5 H  -2.015  -0.002  -0.025   18.25  116.99   28.72    0.094   -0.505   -0.222
 6 H  -1.020   0.020   2.145   20.00  175.87   32.52    1.116    0.987    0.200
 7 H   2.969   0.037   1.974   28.03  -92.19  -15.20   -0.403    0.309    0.449
 8 H  -0.006  -3.047   3.005   32.65 -164.49  -21.31    0.314   -0.160   -0.339
 9 H  -2.103   2.028  -4.128   39.40   47.24   16.98    1.450    0.589   -0.108
10=N   0.022  -2.202   3.294   29.91 -161.71  -10.27
11=N  -1.240  -2.463   2.387   28.16  174.76   -8.21
12=N   2.397   3.539  -3.385   45.87  -11.10    4.20
13 H   4.021   2.988   2.962   42.01  -80.19   15.43    0.006    0.384   -0.431
14 H  -2.016  -0.994   4.059   40.88  175.06   21.34    0.606    0.128    0.172
15 H  -3.102   1.006  -2.057   32.45   80.87   27.38    1.064    0.276   -0.204
16 H   5.002  -0.977   2.046   53.21  -86.15  -28.91   -0.031   -0.258    0.369
17=N   5.243   2.073  -0.883   56.07  -47.96  -14.29
18 H   0.995   0.028   2.835   20.60 -132.26   10.90   -1.186    1.238   -0.143
19 H   3.001   1.998   1.009   27.53  -64.91    5.98    0.004   -0.133    0.021
20 H   2.915   0.974   1.922   26.66  -85.28   -2.07   -0.890    0.308   -0.107
21=N   3.033   0.778   1.601   27.04  -81.43   -7.94
22 H  -0.037  -3.003   1.936   26.76 -167.91  -32.34   -0.292   -0.810   -0.455
23=N   0.983   0.933   3.620   26.57 -132.00   27.68
24=N   0.106   0.042   3.785   27.99 -153.42   22.76
25 H  -0.954   1.959  -1.940   22.27   38.80   31.47   -0.678   -0.440    0.092
26 H   1.934  -3.001   2.965   37.81 -134.07  -33.57   -0.526   -0.660   -0.089
--------------------------------------------------------------------------------
  reciprocal axes matrix [R] (columns)     direct axes matrix [D] (rows)
--------------------------------------------------------------------------------
    0.156885    0.003599    0.062021         4.8452      1.7522     -0.9847
    0.081896    0.072225   -0.135871         1.6062      3.1742      5.2314
   -0.097860    0.146226    0.063400         3.7742     -4.6165      2.1873
--------------------------------------------------------------------------------
c e l l  f o r  EBSD_DAT
--------------------------------------------------------------------------------
a, b, c :      5.2455      6.3264      6.3514
al,be,ga:      85.931      76.028      75.707
  volume:      198.19

Niggli values:     27.5157     40.0229     40.3409
                    2.8509      8.0440      8.1928
--------------------------------------------------------------------------------
results from DIRAX for EBSD_DAT                    Friday 21 May 2021 - 10:17:09
================================================================================
```

For each accepted (type H) reflection, indices h obtained by *DirAx* (Table 3) are related to indices $\mathtt{h}_{Li}$ listed in [1] and Table 1 above by $\pm T\,\mathtt{h} = \mathtt{h}_{Li}$, where

$$T = \begin{bmatrix} -3 & 19 & 17 \\ 2 & -12 & -11 \\ 0 & -1 & -1 \end{bmatrix} .$$

For instance, the reflection 13 has the indices

$$\mathtt{h}_{Li} = \begin{bmatrix} 96 \\ -61 \\ -6 \end{bmatrix} = +T\,\mathtt{h} = T \begin{bmatrix} 4 \\ 3 \\ 3 \end{bmatrix} \approx T \begin{bmatrix} 4.021 \\ 2.988 \\ 2.962 \end{bmatrix} .$$

The $\pm$ sign in front of T is related to the choice of the first edge of a band. The choice determines the direction of the scattering vector.

Table 4: *Ind_X* input file. The lines following the keyword `_Reflections` contain Cartesian components (in Å^{-1}) of the scattering vectors $\boldsymbol{H}_i$ ($i = 1, 2, \ldots, 26$).

```
_NumberOfReflections
        26
_Reflections
 -0.381613    0.245448   -0.040362
 -0.413404   -0.507353    0.056016
  0.444278    0.351223    0.001019
 -0.508321    0.399310    0.078563
 -0.317655   -0.161782    0.195319
 -0.027002   -0.373507    0.238714
  0.588358   -0.022478   -0.159996
  0.174490   -0.628767   -0.254487
 -0.578591    0.535110    0.240619
  0.199885   -0.604781   -0.115379
 -0.055426   -0.603809   -0.087438
  0.178921    0.911853    0.068243
  0.825259    0.142683    0.231164
 -0.068180   -0.788425    0.309236
 -0.610669    0.098132    0.320284
  0.908075    0.061048   -0.502669
  0.775171    0.699036   -0.265922
  0.331995   -0.301704    0.086418
  0.540518    0.253031    0.062502
  0.580123    0.047910   -0.021023
  0.577995    0.087090   -0.081528
  0.103485   -0.482924   -0.312692
  0.382132   -0.344033    0.269722
  0.251451   -0.502520    0.235751
 -0.262867    0.326993    0.256804
  0.476508   -0.461288   -0.440052

_MinMaxVolumeOfPrimitiveCell
    100.0  1000.0
_TheMainCriterion
     0.24
_MaxAllowedMillerIndex
      8
```

Table 5: The best solution from the *Ind_X* output file.

```
  Direct basis vectors (in rows) = inverse of UB matrix;
  transforms RL vectors to Miller indices :
             4.84988326    1.72853023   -0.92048409
             3.74058721   -4.59675207    2.19643448
             1.63027287    3.14144189    5.26309708

       |   h   k   l |      Real (hkl)       |  Error
-------------------------------------------------------
  1    |             |  -1.39  -2.64  -0.06  |  0.531
  2  H- |  -3   1  -2 |  -2.93   0.91  -1.97  |  0.116
  3  -h |   3   0   2 |   2.76   0.05   1.83  |  0.296
  4    |             |  -1.85  -3.56   0.84  |  0.489
  5  H- |  -2   0   0 |  -2.00  -0.02   0.00  |  0.016
  6  -h |  -1   2   0 |  -1.00   2.14   0.04  |  0.146
  7  H- |   3   2   0 |   2.96   1.95   0.05  |  0.076
  8  H- |   0   3  -3 |  -0.01   2.98  -3.03  |  0.035
  9  H- |  -2  -4   2 |  -2.10  -4.10   2.00  |  0.140
 10    |             |   0.03   3.27  -2.18  |  0.330
 11    |             |  -1.23   2.38  -2.45  |  0.629
 12
 13  H- |   4   3   3 |   4.04   2.94   3.01  |  0.072
 14  H- |  -2   4  -1 |  -1.98   4.05  -0.96  |  0.066
 15  H- |  -3  -2   1 |  -3.09  -2.03   1.00  |  0.093
 16  H- |   5   2  -1 |   4.97   2.01  -0.97  |  0.040
 17  -h |   5  -1   2 |   5.21  -0.90   2.06  |  0.243
 18  -h |   1   3   0 |   1.01   2.82   0.05  |  0.188
 19  H- |   3   1   2 |   3.00   1.00   2.01  |  0.007
 20  H- |   3   2   1 |   2.92   1.90   0.99  |  0.129
 21    |             |   3.03   1.58   0.79  |  0.470
 22  H- |   0   2  -3 |  -0.05   1.92  -2.99  |  0.092
 23    |             |   1.01   3.60   0.96  |  0.399
 24  -h |   0   4   0 |   0.13   3.77   0.07  |  0.277
 25  H- |  -1  -2   2 |  -0.95  -1.92   1.95  |  0.107
 26  H- |   2   3  -3 |   1.92   2.94  -2.99  |  0.104
-------------------------------------------------------
  19h and  14H vectors out of  26.    Quality : 0.673

 Primitive cell :
                         5.230    6.320    6.342
                        85.40    75.17    75.68

 Volume of the cell  :      196.35

 -------------------------------------------------------
```

For an individual (type `H-` or `-h`) reflection, indices `h` listed in Table 5 are related to the indices $\mathtt{h}_{Li}$ by $\pm T\,\mathtt{h} = \mathtt{h}_{Li}$, where

$$T = \begin{bmatrix} -3 & 17 & 19 \\ 2 & -11 & -12 \\ 0 & -1 & -1 \end{bmatrix} .$$

The only exception is the reflection 24 with the indices related via $+T\,\mathtt{h} = 2\,\mathtt{h}_{Li}$.

Table 6: *IndX_Laue* input file. The lines following the keyword `_Reflections` contain Cartesian components of normalized scattering vectors $\boldsymbol{H}_i/|\boldsymbol{H}_i|$ $(i = 1, 2, \ldots, 26)$.

```
_NumberOfReflections
        26
_Reflections
 -0.837745    0.538825   -0.088605
 -0.629377   -0.772406    0.085280
  0.784472    0.620162    0.001799
 -0.780638    0.613227    0.120650
 -0.781473   -0.398006    0.480511
 -0.060801   -0.841051    0.537529
  0.964302   -0.036841   -0.262229
  0.249130   -0.897727   -0.363346
 -0.702157    0.649390    0.292006
  0.308787   -0.934281   -0.178241
 -0.090473   -0.985618   -0.142729
  0.192028    0.978652    0.073242
  0.949862    0.164226    0.266067
 -0.080245   -0.927951    0.363962
 -0.876754    0.140890    0.459840
  0.873390    0.058716   -0.483469
  0.719649    0.648967   -0.246875
  0.726702   -0.660396    0.189160
  0.900750    0.421665    0.104157
  0.995958    0.082252   -0.036092
  0.979358    0.147565   -0.138142
  0.177033   -0.826144   -0.534925
  0.658131   -0.592515    0.464532
  0.412641   -0.824654    0.386876
 -0.534384    0.664747    0.522059
  0.598686   -0.579564   -0.552884

_ExtentOfTheSearch
   9
_AngularDeviationCriterion
   2.0
_MaxAllowedMillerIndex
   8
```

Table 7: The best solution from the *IndX_Laue* output file.

```
  Direct basis vectors (in rows) = inverse of UB matrix;
  transforms RL vectors to Miller indices :
           -0.81431575   -0.30540891    0.19624090
           -0.26822567   -0.55078048   -0.89243546
           -0.63065968    0.80708863   -0.35715601

       |   h   k   l |      Real (hkl)       |  Error
-------------------------------------------------------------
  1  H- |   1   0   2 |   1.00   0.01   2.00  |  0.015
  2  H- |   3   2  -1 |   2.98   2.02  -1.00  |  0.026
  3  H- |  -3  -2   0 |  -3.00  -2.00   0.02  |  0.019
  4  H- |   2  -1   4 |   2.00  -1.00   4.00  |  0.000
  5  H- |   1   0   0 |   1.00   0.00   0.00  |  0.000
  6  H- |   1   0  -2 |   0.99   0.00  -2.00  |  0.009
  7  H- |  -3   0  -2 |  -3.01  -0.02  -1.98  |  0.024
  8  H- |   0   1  -1 |   0.00   1.00  -1.00  |  0.000
  9  H- |   1  -1   2 |   1.00  -1.00   2.00  |  0.003
 10  H- |   0   2  -3 |   0.00   2.00  -3.00  |  0.004
 11  H- |   1   2  -2 |   1.00   2.01  -1.99  |  0.015
 12  H- |  -2  -3   3 |  -2.03  -3.02   2.96  |  0.055
 13  H- |  -4  -3  -3 |  -4.02  -3.04  -2.93  |  0.085
 14  H- |   2   1  -4 |   2.02   1.00  -3.99  |  0.026
 15  H- |   3  -1   2 |   3.01  -1.00   1.99  |  0.017
 16  H- |  -5   1  -2 |  -5.00   1.00  -2.01  |  0.006
 17  H- |  -5  -2   1 |  -5.01  -1.99   0.95  |  0.051
 18  H- |  -1   0  -3 |  -1.00   0.00  -3.00  |  0.000
 19  H- |  -3  -2  -1 |  -3.00  -2.02  -0.95  |  0.059
 20  H- |  -3  -1  -2 |  -3.02  -1.00  -1.97  |  0.040
 21  H- |  -4  -1  -2 |  -3.97  -1.01  -2.05  |  0.059
 22  H- |   0   3  -2 |   0.01   3.00  -1.99  |  0.013
 23  H- |  -1  -1  -4 |  -1.00  -1.00  -4.00  |  0.004
 24  H- |   0   0  -1 |  -0.01   0.00  -1.00  |  0.008
 25  H- |   1  -2   2 |   0.98  -2.01   2.00  |  0.026
 26  H- |  -2   3  -3 |  -1.95   3.03  -3.01  |  0.062
-------------------------------------------------------------
Odd [%] |  31  25  19 |
-------------------------------------------------------------
  26h and  26H vectors out of  26.    Quality : 1.000

 Primitive cell :
                          8.916   10.825   10.848
                         87.88    78.25    77.34

 Volume of the cell  :     1000.00

 -------------------------------------------------------
```

The scaling factor determined using the algorithm described in Appendix A is $S = 5.78807$Å. The corresponding volume of the cell is $V = S^3 = 193.91$Å^3. With the default volume of 1000Å^3 used by *IndX_Laue*, the parameters a, b and c resulting from *IndX_Laue* need to be multiplied by $(193.91/1000)^{1/3} = 0.578807$. Thus, the primitive cell parameters are $a = 5.161$, $b = 6.266$ and $c = 6.279$. The integers m determining the order of reflections are

equal to 1 in all cases except the reflections 5, 8, 9 and 24 for which they are 2, 3, 2 and 4, respectively. The relationship between the resulting reflection indices $\mathtt{h}$ and the indices $\mathtt{h}_{Li}$ is $\pm T\,\mathtt{h} = \mathtt{h}_{Li}$, where

$$T = \begin{bmatrix} -3 & 19 & 17 \\ 2 & -12 & -11 \\ 0 & -1 & -1 \end{bmatrix} .$$

The only exception is the reflection 24 with the indices related via $-T\,\mathtt{h} = 2\,\mathtt{h}_{Li}$.

On recommendation of an anonymous reviewer, below is a derivation of the formula for determination of the scattering vector $\boldsymbol{H}$ from positions of edges of an EBSD band.

Let $\boldsymbol{k}_0$ and $\boldsymbol{k}$ denote the wave vectors of the incident and the diffracted beams, respectively. The derivation is based on the Laue equation $\boldsymbol{H} = \boldsymbol{k} - \boldsymbol{k}_0$ and the condition $\boldsymbol{k}^2 = \boldsymbol{k}_0^2$ $(= 1/\lambda^2)$ arising from energy conservation[1]. Edges of EBSD bands are generated by divergent beams, i.e., directions of the vectors $\boldsymbol{k}_0$ are arbitrary. The formula governing the wave vectors of diffracted beams is obtained by eliminating $\boldsymbol{k}_0$; one has

$$\boldsymbol{H} \cdot (\boldsymbol{H} - 2\boldsymbol{k}) = (\boldsymbol{k} - \boldsymbol{k}_0) \cdot ((\boldsymbol{k} - \boldsymbol{k}_0) - 2\boldsymbol{k}) = \boldsymbol{k}_0^2 - \boldsymbol{k}^2 = 0 \ .$$

Thus, the wave vectors $\boldsymbol{k}$ corresponding to the scattering vector $\boldsymbol{H}$ are on the cone described by $\boldsymbol{H} \cdot (\boldsymbol{H} - 2\boldsymbol{k}) = 0$. Similarly, the wave vectors corresponding to $-\boldsymbol{H}$ are on the cone $(-\boldsymbol{H}) \cdot ((-\boldsymbol{H}) - 2\boldsymbol{k}) = \boldsymbol{H} \cdot (\boldsymbol{H} + 2\boldsymbol{k}) = 0$. Let the wave vector $\boldsymbol{k}_1$ be on the first cone and and $\boldsymbol{k}_2$ on the second cone, i.e.,

$$\boldsymbol{H} \cdot (\boldsymbol{H} - 2\boldsymbol{k}_1) = 0 \ , \quad \boldsymbol{H} \cdot (\boldsymbol{H} + 2\boldsymbol{k}_2) = 0 \ .$$

By adding and subtracting the sides of these equations, one gets

$$\boldsymbol{H} \cdot (\boldsymbol{H} - (\boldsymbol{k}_1 - \boldsymbol{k}_2)) = 0 \ , \quad \boldsymbol{H} \cdot (\boldsymbol{k}_1 + \boldsymbol{k}_2) = 0 \ . \tag{1}$$

If $\boldsymbol{H}$, $\boldsymbol{k}_1$ and $\boldsymbol{k}_2$ are coplanar, one can express the scattering vector as a linear combination of $\boldsymbol{k}_1$ and $\boldsymbol{k}_2$. With $\boldsymbol{H} = \alpha_1 \boldsymbol{k}_1 + \alpha_2 \boldsymbol{k}_2$, eqs.(1) can be written in the form

$$\boldsymbol{H} \cdot ((\alpha_1 \boldsymbol{k}_1 + \alpha_2 \boldsymbol{k}_2) - (\boldsymbol{k}_1 - \boldsymbol{k}_2)) = 0 \ , \quad (\alpha_1 \boldsymbol{k}_1 + \alpha_2 \boldsymbol{k}_2) \cdot (\boldsymbol{k}_1 + \boldsymbol{k}_2) = 0 \ .$$

Using $\boldsymbol{H} \cdot \boldsymbol{k}_1 = \boldsymbol{H}^2/2$ and $\boldsymbol{H} \cdot \boldsymbol{k}_2 = -\boldsymbol{H}^2/2$, one obtains

$$(\alpha_1 - \alpha_2 - 2)\boldsymbol{H}^2 = 0 \ , \quad (\alpha_1 + \alpha_2)(1/\lambda^2 + \boldsymbol{k}_1 \cdot \boldsymbol{k}_2) = 0 \ . \tag{2}$$

Both $\boldsymbol{H}^2$ and $1/\lambda^2 + \boldsymbol{k}_1 \cdot \boldsymbol{k}_2$ are positive for physical reasons, and this means that eqs.(2) are solved by $\alpha_1 = 1$ and $\alpha_2 = -1$. Thus, the scattering vector can be expressed as

$$\boldsymbol{H} = \boldsymbol{k}_1 - \boldsymbol{k}_2 = (\widehat{\boldsymbol{k}}_1 - \widehat{\boldsymbol{k}}_2)/\lambda \ , \tag{3}$$

where $\widehat{\boldsymbol{k}}_j = \boldsymbol{k}_j/|\boldsymbol{k}_j| = \lambda \boldsymbol{k}_j$ $(j = 1, 2)$, and the vectors $\widehat{\boldsymbol{k}}_1$ and $\widehat{\boldsymbol{k}}_2$ are coplanar with $\boldsymbol{H}$. When $\widehat{\boldsymbol{k}}_j$ is directed toward the foot of the perpendicular from the pattern center of the j-th edge, the condition of coplanarity is satisfied. Thus, knowing the vectors $\widehat{\boldsymbol{k}}_j$ for the band edges and the wavelength λ, one can determine the scattering vector corresponding to the band by using eq.(3).

References

[1] Lili Li and Ming Han. Determining the Bravais lattice using a single electron backscatter diffraction pattern. *J. Appl. Cryst.*, 48:107–115, 2015.

[1] Formation of EBSD patterns involves inelastic scattering but the energy loss is negligible.